Journal of Solution Chemistry (2019) 48:1266–1286
https://doi.org/10.1007/s10953-019-00913-y

Method of UV-Metric and pH-Metric Determination of Dissociation Constants of Ionizable Drugs: Valsartan

Milan Meloun[1] · Lucie Pilařová[1] · Aneta Pfeiferová[1] · Tomáš Pekárek[2]

Received: 22 November 2018 / Accepted: 30 April 2019 / Published online: 10 September 2019

Abstract

Valsartan is used for treating high blood pressure, congestive heart failure and to increase the chances of living longer after a heart attack and to reduce the mortality rate for people with left ventricular dysfunction following a heart attack. Regression analysis of the pH-spectra with REACTLAB and of the pH-titration curve with ESAB determined two close consecutive dissociation constants. MARVIN and ACD/Percepta predicted two protonation sites. In water a soluble anion L^{2-} forms two sparingly soluble species LH^{-}, LH_2. Although adjusted pH less affected the spectral changes in the chromophore, $pK^{T}_{a1} = 3.70 \pm 0.12$, $pK^{T}_{a2} = 4.82 \pm 0.08$ at 25 °C and $pK^{T}_{a1} = 3.44 \pm 0.08$, $pK^{T}_{a2} = 4.67 \pm 0.02$ at 37 °C in an aqueous phosphate buffer were determined. By regression analysis of potentiometric pH-titration curves and $pK^{T}_{a1} = 3.51 \pm 0.01$, $pK^{T}_{a2} = 4.63 \pm 0.01$, at 25 °C and $pK^{T}_{a1} = 3.44 \pm 0.03$, $pK^{T}_{a2} = 4.51 \pm 0.03$ at 37 °C in an aqueous medium were estimated. Positive enthalpy values $\Delta H^0(pK_{a1}) = 10.33$ kJ·mol^{-1}, $\Delta H^0(pK_{a2}) = 17.70$ kJ·mol^{-1} showed that the dissociation process was endothermic. The standard state Gibbs energy changes are $\Delta G^0(pK_{a1}) = 20.03$ kJ·mol^{-1}, $\Delta G^0(pK_{a2}) = 26.43$ kJ·mol^{-1} at 25 °C and the ΔS^0 at 25 °C and 37 °C are ($\Delta S^0(pK_{a1}) = -32.56$ J·K^{-1}·mol^{-1}, $\Delta S^0(pK_{a2}) = -29.26$ J·K^{-1}·mol^{-1} at 25 °C and $\Delta S^0(pK_{a1}) = -30.01$ J·K^{-1}·mol^{-1}, $\Delta S^0(pK_{a2}) = -25.92$ J·K^{-1}·mol^{-1} at 37 °C.

Electronic supplementary material The online version of this article (https://doi.org/10.1007/s10953-019-00913-y) contains supplementary material, which is available to authorized users.

✉ Milan Meloun
milan.meloun@upce.cz

[1] Department of Analytical Chemistry, University of Pardubice, 532 10 Pardubice, Czech Republic

[2] Zentiva k.s, U kabelovny 130, 102 37 Prague, Czech Republic

Graphic Abstract

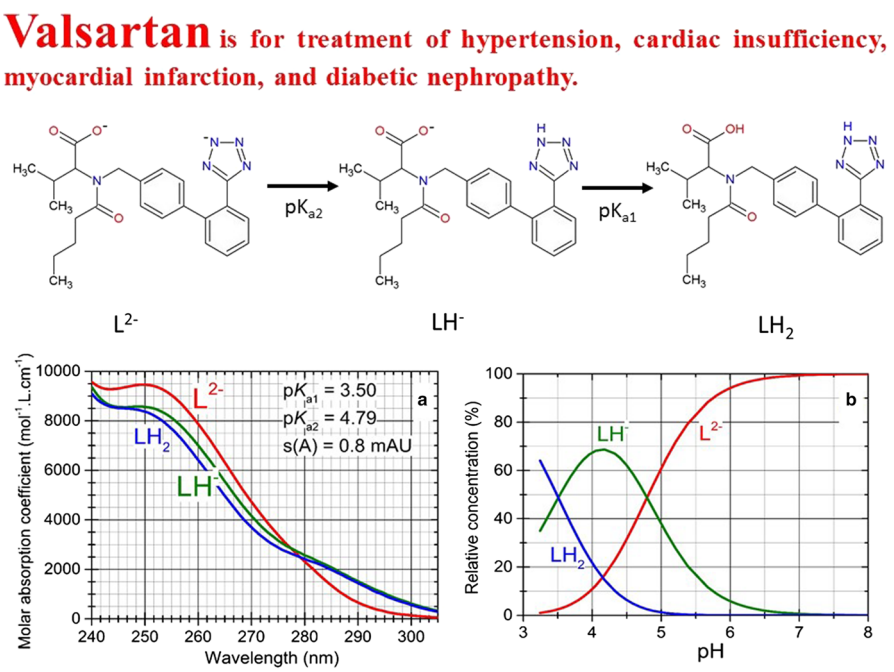

Keywords Dissociation constants · Valsartan · Spectrophotometric titration · pH-titration · REACTLAB · SQUAD84 · ESAB

1 Introduction

Angiotensin II receptor blockers (ARB), also known as sartans, represent an important class of drugs used in the treatment of hypertension, cardiac insufficiency, myocardial infarction, and diabetic nephropathy [1]. Valsartan (trade name Diovan, Novartis International AG) is mainly used for treating high blood pressure, congestive heart failure, and to increase the chances of living longer after a heart attack [1, 2]. It is an angiotensin II receptor antagonist, commonly called an ARB, or angiotensin receptor blocker, that is selective for the type I (AT_1) angiotensin receptor [3]. Valsartan is also used to reduce the mortality rate for people with left ventricular dysfunction following a heart attack [4]. In people with type II diabetes and high blood pressure or albumin in the urine, Valsartan is used to slow the development and worsening of end-stage kidney disease [5]. Valsartan blocks the actions of angiotensin II, which include constricting blood vessels and activating aldosterone, to reduce blood pressure [6].

Its IUPAC name and formula are (*S*)-3-methyl-2-(*N*-[[2′-(2H-1,2,3,4-tetrazol-5-yl) biphenyl-4-yl]methyl]pentan amido)butanoic acid and $C_{24}H_{29}N_5O_3$: it has a molar mass 435.528 g·mol^{-1}, a melting point of 116–117 °C, and a solubility in water of 1.406 mg·L^{-1} at 25 °C. It is soluble in ethanol and methanol (23.4 mg·L^{-1}). Valsartan is a diprotic acid with a carboxylic acid group and a tetrazole ring (Fig. 1). Grujič et al.

[1] potentiometrically determined the pK_a values of the examined sartans: pK_{a1} 3.88 and pK_{a2} 4.55 for Irbesartan, pK_{a1} 3.27 and pK_{a2} 4.60 for Losartan, and pK_{a1} 3.79 (imidazol) and pK_{a2} 4.55 (tetrazol) for Valsartan. The close values of the two consecutive ionization constants point out to an overlapped protolytic equilibrium, which significantly complicates attribution of the pK_a values to the corresponding ionizable centers. Knowledge of the pK_a values of drugs is required to perform tests of biopharmaceutical characterization, and in developing new pharmaceutical formulations or improving the available ones [1]. Defining the ionization profile of drugs is particularly significant for prediction of their behavior under physiological conditions where the ionization state strongly affects the solubility of drugs at the application site and their ability to diffuse through biological membranes [7].

One of the most important physico-chemical characteristics of every drug is its pK_a value. The dissociation constant pK_{ai} of the acid LH_j can be determined by a regression analysis of potentiometric titration data also called the pH-metric analysis where the common parameters (pK_{ai}, $i=1, \ldots, j$) and the group parameters (E^0, L_0, H_T) are simultaneously refined. The non-linear regression programs for analyzing potentiometric pH-titration data, ESAB [8], SUPERQUAD and HYPERQUAD [9, 10], have been used, cf. Ref. [11–13].

Spectrophotometric UV-metric spectra analysis [14] is a highly sensitive and convenient method for determining pK_a values in very dilute aqueous solutions since it requires relatively simple equipment and can work with a sub-micromolar compound concentration (about 10^{-5} to 10^{-6} mol·dm^{-3}) [15–17].

The accuracy of theoretical predictions of pK_a from the molecular structure with the use of two predictive programs ACD/Percepta [18–21] and MARVIN [22] was found to be the best of all nine available programs [23–25].

The aim of our study was to carry out the regression analysis of the pH-absorbance matrix with small absorbance changes in the spectra of Valsartan and also to carry out a pH-metric potentiometric determination of the protonation model to find suitable conditions for a reliable regression determination of all close consecutive dissociation constants and to calculate the thermodynamic parameters such as the enthalpy, entropy and Gibbs energy.

Valsartan, $C_{24}H_{29}N_5O_3$

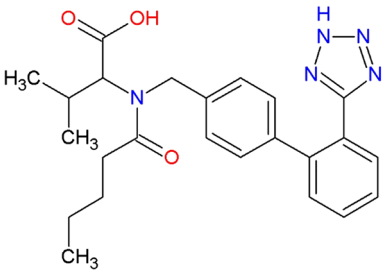

Fig. 1 Structural formula of Valsartan

2 Computational Details

To implement equilibrium hard-modeling of spectrophotometric titration data, the analyst must make a variety of crucial data processing choices that address negative absorbance and molar absorptivity values. A detailed tutorial of UV–VIS pH-titration [26] also called the UV-metric spectra analysis [14], and alternatively the pH-metric analysis have been applied and were described previously in the ten steps procedure [26].

3 Experimental Section

3.1 Chemicals and Solutions

Valsartan was donated by ZENTIVA k. s., (Prague) had a declared purity, checked by a HPLC and alkalimetrically, > 99%. This drug was weighed straight into a reaction vessel, resulting in a concentration of about 1.0×10^{-4} mol·dm^{-3}.

Hydrochloric acid, 1 mol·dm^{-3}, was prepared by diluting a concentrated HCl (p. a., Lachema Brno) with redistilled water and standardization against HgO and KI, with a reproducibility better than 0.002, according to the equation $HgO + 4KI + H_2O \rightleftharpoons 2KOH + K_2[HgI_4]$ and $KOH + HCl \rightleftharpoons KCl + H_2O$. Potassium hydroxide, 1 mol·dm^{-3}, was prepared from the exact weight of pellets p.a., Aldrich Chemical Company with carbon-dioxide-free redistilled water kept for 50 min prior to use in an ultrasonic bath. The solution was stored for several days in a polyethylene bottle under an argon atmosphere. This solution was standardized against a solution of potassium hydrogen-phthalate using the derivative method with reproducibility 0.001.

Mercury oxide, potassium iodide and potassium chloride, p.a. Lachema Brno were not extra purified. Twice-redistilled water, kept for 50 min prior to use in a sonographic bath, was used in the preparation of solutions [27–31].

3.2 Apparatus

The apparatus used and both titration procedures have been described in detail [27–30]. The free hydrogen-ion concentration [H^+] was measured using a Hanna HI 3220 digital voltmeter having a precision of ±0.002 pH units, using the Theta HC 103-VFR combined glass electrode. The potentiometric titrations of the drug with potassium hydroxide were performed using a hydrogen activity scale. Standardization of the pH meter was performed using WTW standard buffers values, 4.006 (4.024), 6.865 (6.841) and 9.180 (9.088) at 25 °C and 37 °C, respectively, in brackets.

The spectrophotometric multiple-wavelength pH-titration was carried out as follows: an aqueous solution 20.00 cm^3 containing 10^{-5} mol·dm^{-3} drug, 0.100 mol·dm^{-3} hydrochloric acid and 10 cm^3 KCl solution, for adjustment of ionic strength, was titrated with standard 1.0 mol·dm^{-3} KOH at 25 °C and 37 °C, respectively, and 80 absorption spectra were recorded. Titrations were performed in a water-jacketed double-walled glass vessel of 100 mL volume, closed with a Teflon bung containing the electrodes, an argon inlet, a thermometer, a propeller stirrer and a capillary tip from a micro-burette. All pH measurements were carried out at 25.0 ± 0.1 °C and 37.0 ± 0.1 °C. When the drug was titrated, a stream of argon gas was bubbled through the solution both to stir and to maintain an

inert atmosphere. The argon was passed through aqueous ionic medium by prior passage through one or two vessels also containing the titrand medium before entering the corresponding titrand solution. The burettes used were syringe micro-burettes of 1250 μL capacity (META, Brno) with a 25.00 cm micrometer screw, [26]. The polyethylene capillary tip of the micro-burette was immersed in the solution when adding reagent but pulled out after each addition to avoid leakage of the reagent during the pH reading. The micro-burette was calibrated by ten replicate determinations of the total volume of delivered water by weighing on a Sartorius 1712 MP8 balance with results evaluated statistically, leading to a precision of ±0.015% in the added volume over the whole volume range. The solution was pumped into the cuvette and spectrophotometric measurement was performed with the use of a Cintra 40 (GBC, Australia) spectrophotometer.

3.3 Software

An estimation of the dissociation constants was performed by the nonlinear regression analysis of the UV-metric spectra analysis using SQUAD84 [16], REACTLAB [32] programs and of potentiometric pH-metric titration data using the ESAB program [8], and by spectra interpretation using the INDICES program [33]. Most graphs were plotted using ORIGIN 9.1, [34]. The programs ACD/Percepta [18] and MARVIN [22] for predictions of pK_a values were based on the structural formulae of drug compounds.

4 Results

The methods of numerical analysis of pH-spectra and potentiometric pH-titration curves have proven to be the best instrumental methods because they reliably determine even close consecutive dissociation constants, also in case of poorly soluble drugs. The pH-spectroscopic titration (the UV-metric method) has been used as an alternative method to the potentiometric pH-titration (the pH-metric method) of dissociation constants with large molar absorption coefficients due to its high sensitivity to the concentration of the substance, even at concentrations as low as 10^{-5} mol·dm^{-3}.

4.1 UV-Metric Spectral Analysis

The experimental procedure and computational strategies for determining dissociation constants by analyzing the pH-absorbance matrix were described in the 10 steps procedure in the previously published tutorial [26] and also on the page 226 of Ref. [11]. In addition to determining the number of protonation equilibria, the number of differently protonated species, the speciation diagram, and the graph of the molar absorption coefficients within the range of measured wavelengths, statistical reliability criteria along with statistical tests of the protonation model found should be included.

4.1.1 Step 1: Theoretically Predicted pK_a of the Valsartan

The first step of data analysis was the prediction of dissociation constants, based on a quantum-chemical calculation and concerned on the structural pattern of the studied drug´s molecule. Valsartan is a diprotic acid with carboxylic group and tetrazole ring (Fig. 1). The

prediction program MARVIN has identified two protonizable centers A and B for Valsartan, which could be theoretically associated with up to two predicted dissociation constants (Fig. 2). The prediction programs MARVIN, PALLAS and ACD/Percepta predicted dissociation constants slightly different, so it was obvious that experimental determination would offer the more reliable results.

4.1.2 Step 2: The Number of Light-Absorbing Species n_c

Before analysis of absorbance spectra, the raw data should be filtered using singular value decomposition. This technique is based on the observation that, if a spectra dataset consists of contributions from r absorbing chemical species, then the first r factors of the absorbance matrix contain the vast majority of the chemical information obtained by the experiment. The quantity r is referred to as the matrix rank, and in general, r should be less than or equal to m, where m is the number of chemical species. Most simply, inspection of the eigenvalues of the data matrix often reveals that the first factors have large significances until a cutoff in the Cattel graph, after which the factors have small significances. These latter factors may be taken to principally represent the spectrometer noise that nonetheless contributes mathematically to the spectra. By removing these factors from the data, it may fit the model to the chemical information with reduced noise from causes beyond chemical equilibria and Beer's law for additive absorbance.

The Cattel index graph of singular values (Fig. 3) showed that the entire set of spectra of Valsartan at the wavelengths of 240–305 nm was able to indicate three light absorbing species in the mixture $n_c = k^* = 3$ with the experimental noise level $s_{inst}(A) = 1.0$ mAU, even though the molar absorption coefficients of the first pair of species LH^- and LH_2 were quite similar. The true number of light-absorbing species separated from spectral noise could be correctly evaluated with the non-linear regression analysis.

4.1.3 Step 3: The Protonation Model Building and Testing

Using the program REACTLAB, nonlinear regression analysis was applied in the absorbance spectra treatment, i.e. the application of the regression triplet method (data critique, model critique and method critique), cf. Ref. [12, 13]. Finding the best hypothesis for a

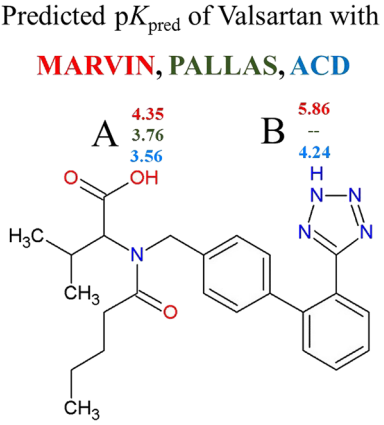

Fig. 2 Molecular structure of Valsartan with highlighted protonation centers A and B and predicted pK_a values using programs MARVIN, PALLAS and ACD/Percepta

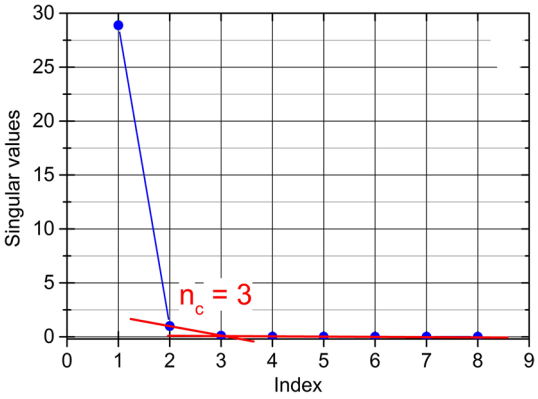

Fig. 3 Using Cattel index graph with the residual standard deviation $s_k(A)$, the rank of the absorbance matrix is $k^* = 3$ for Valsartan or the number of species is equal to $n_c = 3$. (INDICES in S-PLUS), [33]

protonation model containing one, two or three dissociation constants is shown in the graphs of the molar absorption coefficients (Fig. 4a) and the distribution diagrams of all the differently protonated species (Fig. 4b) for the proposed hypothesis of the protonation model.

The design and building of the protonation model involves the decision-making process for accepting the calculated parameters with some statistical diagnostics for the proposed hypothesis of the protonation model. It has been shown that the building of the Valsartan protonation model was not an easy task because this drug had two close together, consecutive dissociation constants ($\left| pK_{a2} - pK_{a1} \right| < 3$) as well as the fact that the pH slightly affected the changes in the absorbance values of chromophores. Both dissociation constants were ill-conditioned in a regression model and their determination was therefore uncertain.

The best criterion for testing a hypothesis in regression model building is the fitness test of the calculated spectra through the experimental points of the absorbance matrix, which could be often simplified to the standard deviation of the absorbance after a regression termination.

$$s(A) = \sqrt{RSS/(n-m)} \tag{1}$$

where n is the number of experimental points and m is the number of estimated parameters.

In Table 1 the numerical estimates of dissociation constants, computed by the REACTLAB regression program are reported: the residual mean $E\left| e \right|$ [mAU], residual standard deviation $s(e)$ [mAU] showed an excellent goodness-of-fit of calculated spectra through the experimental points of all spectra was achieved for the protonation model with two dissociation constants. Reliability of calculated estimates of regression parameters can be advantageously tested by the following regression diagnostics (Table 1 and Fig. 4) as explained on page 226 in Ref. [11].

4.1.3.1 Physical Significance of Parameter Estimates In the left part of Fig. 4a, the spectra of the molar absorption coefficients of the differently protonated species, ε_L, ε_{LH} and ε_{LH2} of the Valsartan species versus wavelengths are shown. When the pair of ε curves seem to be very similar, the model hypothesis could be uncertain or false.

4.1.3.2 Physical Significance of Species Concentrations The distribution diagram of the relative concentrations of all species (Fig. 4b) shows the protonation equilibria of the differ-

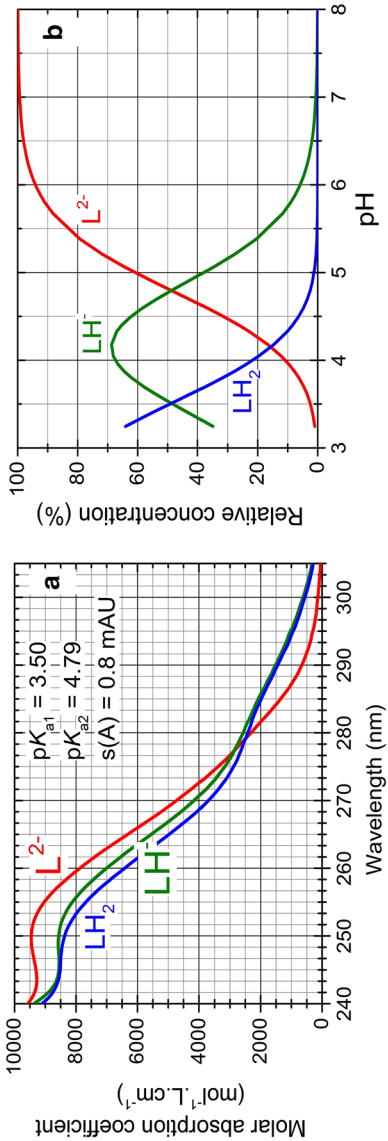

Fig. 4 Building and testing the best protonation model of Valsartan in the pH range from 3 to 8 for the two dissociation constants pK_{a1} and pK_{a2} with the spectra analysis of 1.0×10^{-4} mol·dm^{-3} Valsartan at $I = 0.008$ mol·dm^{-3} and 25 °C. **a** Pure spectral profiles of molar absorption coefficients versus wavelength (nm) for three variously protonated ions of Valsartan. **b** The distribution diagram of the relative concentrations of three variously protonated species depending on pH (REACTLAB, ORIGIN 9)

Table 1 The reproducibility of the best protonation model of Valsartan in the pH range from 12 to 3 for two dissociation constants pK_{a1}, pK_{a2} with REACTLAB at 25 and 37 °C

Temperature		25 °C					37 °C				
Reproducibility		1st set	2nd set	3rd set	4th set	Mean	1st set	2nd set	3rd set	4th set	Mean
Cattel´s scree plot indicating the rank of the absorbance matrix (INDICES)											
Number of spectra measured, n_s		39	29	36	35		34	37	32	39	
Number of wavelengths, n_w		78	78	78	78		78	78	78	78	
Number of light-absorbing species, k^*		3	3	3	3		3	3	3	3	
Estimates of dissociation constants in the searched protonation model											
$pK_{a1}(s_1)$, $LH_2 \rightleftharpoons H^+ + LH^-$	REACTLAB	3.77(00)	3.66(01)	3.66(00)	3.67(00)	3.71 ± 0.05	3.61(01)	3.63(01)	3.51(00)	3.47(00)	3.55 ± 0.08
$pK_{a2}(s_2)$, $LH^- \rightleftharpoons H^+ + L^{2-}$	REACTLAB	4.87(00)	4.84(00)	4.84(00)	4.79(00)	4.83 ± 0.04	4.83(00)	4.80(00)	4.83(00)	4.74(00)	4.79 ± 0.04
Goodness-of-fit test with the statistical analysis of residuals											
Mean residual $E\lvert\bar{e}\rvert$, (mAU)	REACTLAB	0.90	0.70	0.66	0.58		0.64	0.65	0.78	0.89	
Standard deviation of residuals $s(\hat{e})$, [mAU]	REACTLAB	1.17	0.91	0.83	0.75		0.83	0.82	1.04	1.12	
Sigma from REACTLAB, [mAU]	REACTLAB	1.19	0.92	0.84	0.76		0.84	0.83	1.05	1.13	

A solution of 1×10^{-4} mol·dm^{-3} Valsartan at I=0.008 mol·dm^{-3}, for n_s spectra measured at n_w wavelengths for n_z=2, basic components L and H forms variously protonated species. The standard deviations of the parameter estimates are in the last valid digits in parentheses. The resolution criterion and reliability of parameter estimates found are proven with goodness-of-fit statistics such as the mean residual $E\lvert\bar{e}\rvert$ [mAU], the standard deviation of absorbance after termination of the regression process $s(\hat{e})$ [mAU], and the sigma $s(A)$ [mAU] from REACTLAB

ently protonated species L^{2-}, LH^{-}, LH_2. The graph shows that none of the species is minor and all are of physical significance.

4.1.3.3 The Goodness-of-Fit Test The statistical measures of all residuals showed that the minimum of the elliptic hyperparaboloid of the objective RSS function (Table 1) had been reached because the residual mean $E\left|\bar{e}\right|$ [mAU] and the residual standard deviation $s(\hat{e})$ [mAU] reached very low values, <2 mAU, representing $<0.2\%$ of the measured absorbance.

4.1.4 Step 4: The Effective Range of Wavelengths

Two ranges of wavelengths 240–278 nm, 278–308 nm and 240–308 nm were selected and the spectra within these wavelength ranges were evaluated. Figure 5 illustrates the estimates of two dissociation constants including the value of curve fitting expressed here as the standard deviation of absorbance $s(A)$, which served as the reliability criterion of the parameter estimates calculated. The best curve fitting with the fitting criterion $s(A)=0.7$ mAU was achieved in the wavelength range 240–278 nm, although the estimates of the dissociation constants were close in all three tested wavelength ranges. Likewise, the three distribution diagrams of the relative concentration of variously protonated species in Fig. 5 were quite similar.

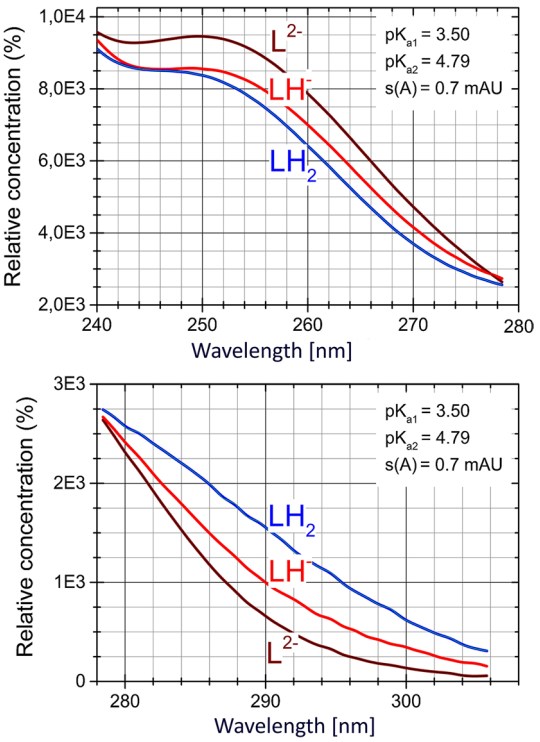

Fig. 5 Search for an effective wavelength range to examine the position of ionizable groups and chromophores to find a sufficient absorbance change in spectrum for adjusted pH, which allows a reliable determination of dissociation constants. The protonation model of two dissociation constants was analyzed using two separate absorption bands. The best fitted spectra were achieved in the 240–280 nm range, although pK_a estimates were the same for all wavelength ranges

4.1.5 Step 5: The Absorbance Change in Spectra within pH Titration

Adjustment of pH did not cause the significant changes in the Valsartan spectrum everywhere, because some chromophores were only slightly affected by pH adjustment. Figure 6a shows a spectrum of the molar absorption coefficients dependences on the wavelength, for three selected wavelengths A through C, for which the *A*–pH curves are displayed. Figure 6b through 6d in the A–C graphs showed a sensitivity of chromophores in the Valsartan molecule to the pH, which was monitored in the form of *A*–pH curves. The maximum changes in absorbance occur for pH changes at 251.1 nm and 266.5 nm (curves A and B). The graphs show the estimates of dissociation constants and the presence of differently protonated species. From these graphs it is also clear that the two dissociation constants were very close and their estimation would be therefore difficult or, sometimes, impossible. Each A–C graph in Fig. 6 also contains the plot of residuals. The quality of the residuals reveals the degree of curve fitness of the calculated *A*–pH curves through the experimental absorbance points. The residuals should oscillate around the zero and their sign should change with frequent oscillations. The residuals should also exhibit a Gaussian distribution with a mean value nearly equal to zero. For the best spectras fitting the standard deviation $s(A)$ is expected to be of the same size as the instrumental noise in absorbance, $s_{\mathrm{inst}}(A)$.

4.1.6 Step 6: The Signal-to-Error Ratio in Spectral Changes

In the spectrophotometric determination of the pK_a values of Valsartan, it was first necessary to investigate whether the adjustment of pH would cause a sufficient absorbance change in the spectrum. It is evident from Fig. 7a, b that the spectral response of the Valsartan molecule is not the same everywhere and sufficient for both protonation equilibria, so it had to be verified whether two dissociation constants could be estimated even with the minimal changes in absorbance. The change for the *i*-th spectrum and the *j*-spectrum absorption can be expressed by the difference relation $\Delta_{ij}=A_{ij}-A_i$. It was necessary to investigate whether these small changes in Δ in the spectra were sufficiently large and greater than the absorbance noise value, expressed here by $s_{\mathrm{inst}}(A)$.

The changes of absorbance difference (mAU) in the spectra were therefore plotted against the pH for all elements of the absorbance matrix (Fig. 7a) and this showed that the absorbance change values were small, but they were still larger than the instrumental noise in Fig. 7b. While residuals *e* in Fig. 7b were predominantly in the range of −1.5 to +1.5 mAU, the changes in absorbance difference in Fig. 7a were in the range of −80 to +120 mAU.

4.1.7 Step 7: The Spectra Deconvolution (Shown in Supplementary Material)

The deconvolution of each experimental spectrum into the absorption bands of the individual species showed whether the protonation hypothesis had been designed efficiently. Figure S1 illustrates the deconvolution of six selected experimental spectra into absorption bands from the differently protonated Valsartan species. At pH = 3.25, the absorption band of the species LH_2, which was in equilibrium with the anion LH^- was still significant. The pH range of 3.80 to 5.07 was very important, because here three species were in equilibrium, namely LH_2, LH^- and L^{2-}. At pH = 5.38 and 5.80, the spectral band of the anion LH^- decreased while the band of L^{2-} increased.

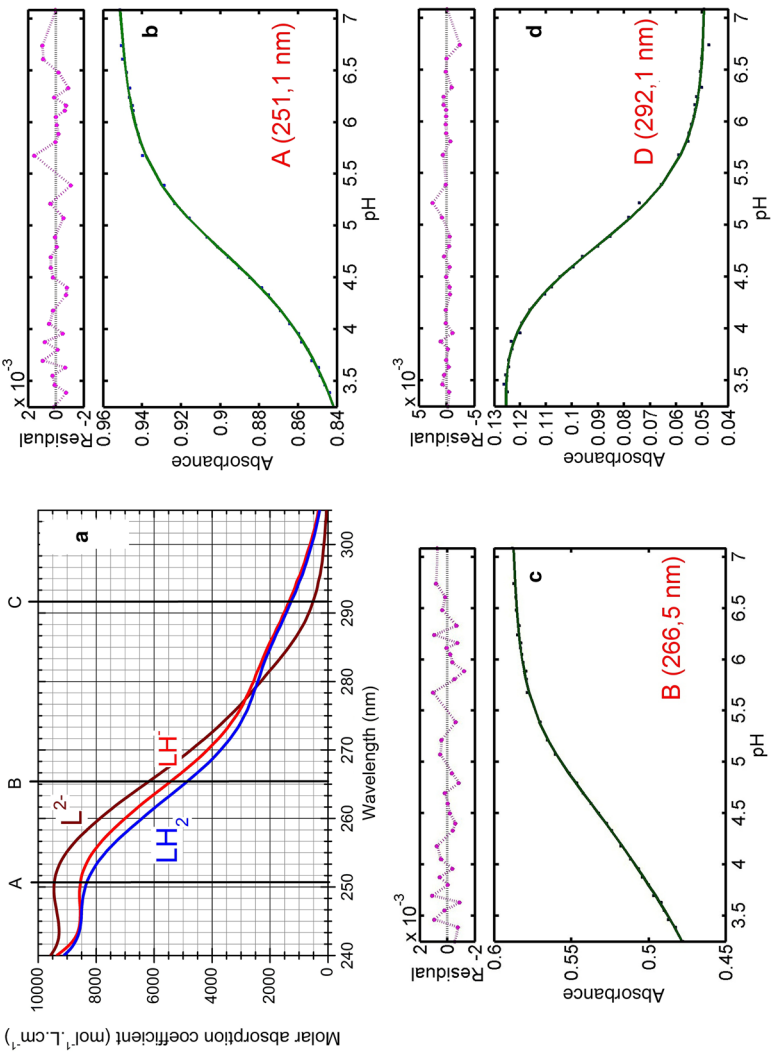

Fig. 6 The adjusted pH did not cause the same absorbance change in the Valsartan spectrum because some chromophores were only slightly affected by pH: **a** the spectrum of the molar absorption coefficient contains positions of four wavelengths A through C for which the *A*–pH curves were analyzed. **b**–**d** the graphs A through C show the sensitivity of chromophores in the Valsartan molecule to pH

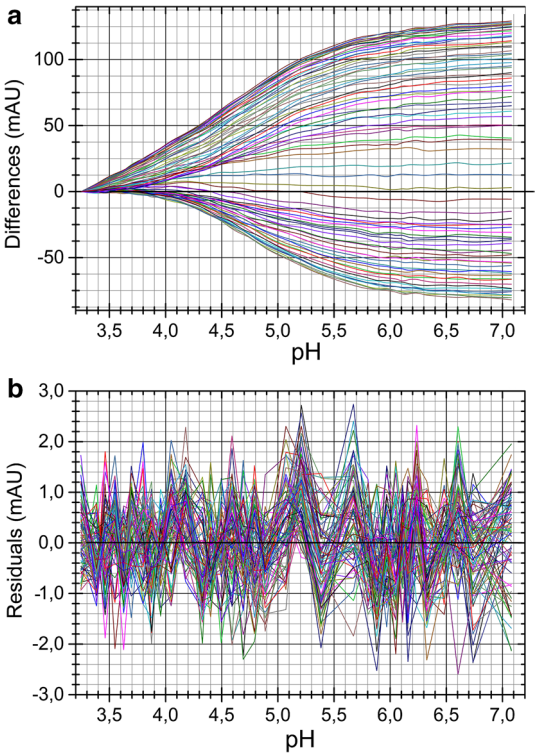

Fig. 7 Analysis of the change Δ_{ij} in absorbance spectra at adjusted pH: **a** the graph of the absorbance change difference Δ_{ij} in the Valsartan spectrum during the pH titration. **b** residuals e [mAU] show whether they were of the same size as the instrumental noise $s_{\text{inst}}(A)$, (REACTLAB, ORIGIN 9)

4.2 Analysis of pH-Metric Data (Shown in Supplementary Material)

The potentiometric titration of the alkalized Valsartan with hydrochloric acid was carried out at 25 °C and 37 °C (Table 2) and at adjusted ionic strength (Fig. S2). In the analysis of pH-metric data, the initial estimate of each dissociation constant of Valsartan was refined using the ESAB program (see Fig. S2).

4.2.1 Step 8: pH-Metric Data Analysed with the Bjerrum Formation Function

Valsartan has two dissociation constants and their refinement was carried out by the nonlinear regression of the pH-metric titration curve using the ESAB program. The nonlinear regression analysis was applied to the central part of the pH-metric titration curve for the deprotonated alkalized with KOH Valsartan being titrated with hydrochloric acid (Fig. S2). Estimates of two dissociation constants pK_{a1} and pK_{a2} were evaluated and plotted using the curve of the Bjerrum formation function. At a higher concentration than 2×10^{-4} mol·dm^{-3}, a precipitate of Valsartan formed. Residuals were defined as the difference between the experimental and the calculated volume of the titrant HCl, $e_i = V_{\text{exp},i} - V_{\text{calc},i}$. The reliability test for the refined dissociation constants estimates was performed by the statistical analysis of the residuals. By refining the group parameters, the statistics of the goodness-of-fit test significantly improved. The relatively sensitive reliability criterion of the estimated dissociation constants was the average of the absolute values of the residuals $E\left|\bar{e}\right|$ [μL]. A comparison of the numerical value of this statistic with the instrumental noise represented

Table 2 ESAB regression refinement of common and group parameters for a pH-metric titration of alkalized 1×10^{-3} mol·dm^{-3} Valsartan titrated with HCl: the estimated dissociation constants pK_{a1}, pK_{a2} of Valsartan when their standard deviations in last valid digit are in parentheses

Temperature	25 °C				37 °C			
Reproducibility	1st set	2nd set	3rd set	4th set	1st set	2nd set	3rd set	4th set
Estimates of the group parameters H_0, H_T and L_0 in the searched protonation model								
Number of points (n)	29	28	29	28	26	24	24	26
$H_0\times100$ (mol·dm^{-3})	5.53(00)	5.55(00)	5.51(00)	5.53(00)	5.49(00)	5.61(00)	5.59(00)	5.72(00)
H_T (mol·dm^{-3})	1.0441	1.0441	1.0441	1.0441	1.0441	1.0441	1.0441	1.0441
$L_0\times1000$ (mol·dm^{-3})	1.18(00)	1.21(00)	1.15(00)	1.24(00)	1.23(00)	1.27(00)	1.26(00)	1.51(00)
Estimates of the common parameters i.e. dissociation constants in the searched protonation model								
pK_{a1}	3.51(01)	3.51(02)	3.51(02)	3.53(02)	3.38(02)	3.36(03)	3.42(02)	3.37(02)
pK_{a2}	4.61(01)	4.61(01)	4.62(01)	4.59(02)	4.46(01)	4.58(02)	4.52(02)	4.56(01)
Goodness-of-fit test with the statistical analysis of residuals								
Arithmetic mean of residuals $E(\hat{e})$ (μL)	1.72×10^{-2}	1.07×10^{-2}	1.38×10^{-2}	1.43×10^{-2}	3.85×10^{-2}	-1.67×10^{-2}	6.67×10^{-2}	1.92×10^{-2}
Median of residuals M (μL)	0.70	0.50	0.60	0.90	0.80	1.00	0.60	0.70
Mean of absolute value of residuals, $E\left\vert\hat{e}\right\vert$ (μL)	0.71	0.69	0.74	0.98	0.79	0.70	0.85	0.86
Residual standard deviation, $s(\hat{e})$, (μL)	0.83	0.84	0.90	1.16	0.93	1.19	1.12	1.08
Residual standard deviation, s_{rel}, (%)	0.00	0.00	0.00	0.00	0.00	−0.00	0.00	0.00
Residual skewness $g_1(\hat{e})$	0.03	0.08	0.03	0.07	0.31	0.88	0.47	0.52
Residual kurtosis $g_2(\hat{e})$	1.96	2.22	2.31	1.96	1.83	2.88	3.13	3.04
Akaike-Information Criterion, *AIC*	−407.95	−393.46	−403.73	−375.20	−359.77	−319.66	−323.71	−351.93
Hamilton R-factor from ESAB (%)	0.07	0.07	0.08	0.11	0.08	0.11	0.10	0.10

The reliability of parameter estimation is proven with a goodness-of-fit statistics: the bias or arithmetic mean of residuals $E(\hat{e})$ (μL), the median (μL), the mean of absolute value of residuals, $E\left\vert\hat{e}\right\vert$ (μL), the standard deviation of residuals $s(\hat{e})$ (μL), the standard deviation of residuals $s_{rel}(\hat{e})$ (%), the residual skewness $g_1(\hat{e})$ and the residual kurtosis $g_2(\hat{e})$ proving a Gaussian distribution, the Hamilton R-factor of relative fitness (%) from ESAB and the Akaike-Information Criterion *AIC*. Common parameters refined: pK_{a1}, pK_{a2}. *Group parameters refined:* H_0, H_T, L_0. *Constants*: $t=25.0$ °C, p$K_w=13.9799$, $s(V)=s_{inst}(y)=0.1$ μL, I_0 adjusted (in vessel), $I_T=1.04477$ (in burette HCl)

here by the instrumental standard deviation of titrant HCl, $s_{inst}(V) = s(V) = 0.1$ μL, has proven an excellent curve fitting, since the mean residual $E\,|\,\bar{e}\,|$ and the residual standard deviations of titrant HCl $s(V)$ were equal or lower than the experimental noise, $s_{inst}(V)$. The values of both monitored statistics here, 0.1 μL, were similar to the instrumental error of the used microburette $s(V) = 0.1$ μL. In addition, the residuals oscillate between the lower (−0.2 μL) and the upper limit (0.2 μL) of the internal Hoaglin boundaries, and no residual value was found outside these limits (see page 81, Ref. [13]). Estimates of dissociation constants refined by the program ESAB were therefore proven to be sufficiently reliable (Table 2). The curve fitting could be improved only by further refining the group parameter L_0, the concentration of the drug Valsartan in the titration vessel.

4.2.2 Step 9: Uncertainty of pK_a in Reproduced Measurements (Shown in Supplementary Material) (Fig. 3S)

The reproducibility of the dissociation constants evaluated with REACTLAB, from four reproduced measurements was found to be in good agreement, as demonstrated in Table 1. The interpretation will be as follows:

(a) An interval estimate of the mean value from four reproduced dissociation constants also served here as the measure of uncertainty for each consecutive dissociation constant.
(b) At 37 °C, the dissociation constant estimates were a little more acidic, i.e., they had lower values of pK_a than those estimates at 25 °C.
(c) Very similar values of two consecutive dissociation constants pK_{a1} and pK_{a2} could result in some difficulties in the minimization or could make the iterative refinement fail. The reasons could be e.g. that an intermediate species was not present at a sufficiently high concentration, or that the too close pK_{a1} or pK_{a2} value of one species was highly correlated with the pK_a value of another species, such those species would each have much the same response to pH.
(d) When the normal equations were singular, one or more of the correlation coefficients between two parameters pK_{a1} and pK_{a2} was equal to one or minus one so that the refinement process could be terminated [12] (see Tables S1, S2).

4.2.3 Step 10: Thermodynamic Dissociation Constants

By applying the Debye–Hückel equation to the data from Tables 1 and 2, the unknown parameters pK^T_{a1} and pK^T_{a2} were estimated at two temperatures of 25 °C and 37 °C (Tables S1, S2). Due to the narrow range and low ionic strength values, which were adjusted with KCl, two parameters, namely the ion-size parameter $\mathring{a}$ and the salting-out coefficient C, could not be calculated. Figure 8 shows an extrapolation of the mixed dissociation constants to zero ionic strength according to the Debye–Hückel limiting law for the protonation model of two dissociation constants at 25 °C and 37 °C using straight lines with the Working–Hotteling 95% confidence bands (cf. p. 474 in Ref. [35]) $pK^T_{a1} = 3.70 \pm 0.12$, $pK^T_{a2} = 4.82 \pm 0.08$ at 25 °C and $pK^T_{a1} = 3.44 \pm 0.08$, $pK^T_{a2} = 4.67 \pm 0.02$ at 37 °C (spectrophotometry) and $pK^T_{a1} = 3.51 \pm 0.00$, $pK^T_{a2} = 4.63 \pm 0.00$, at 25 °C and $pK^T_{a1} = 3.44 \pm 0.03$, $pK^T_{a2} = 4.51 \pm 0.03$ at 37 °C (potentiometry).

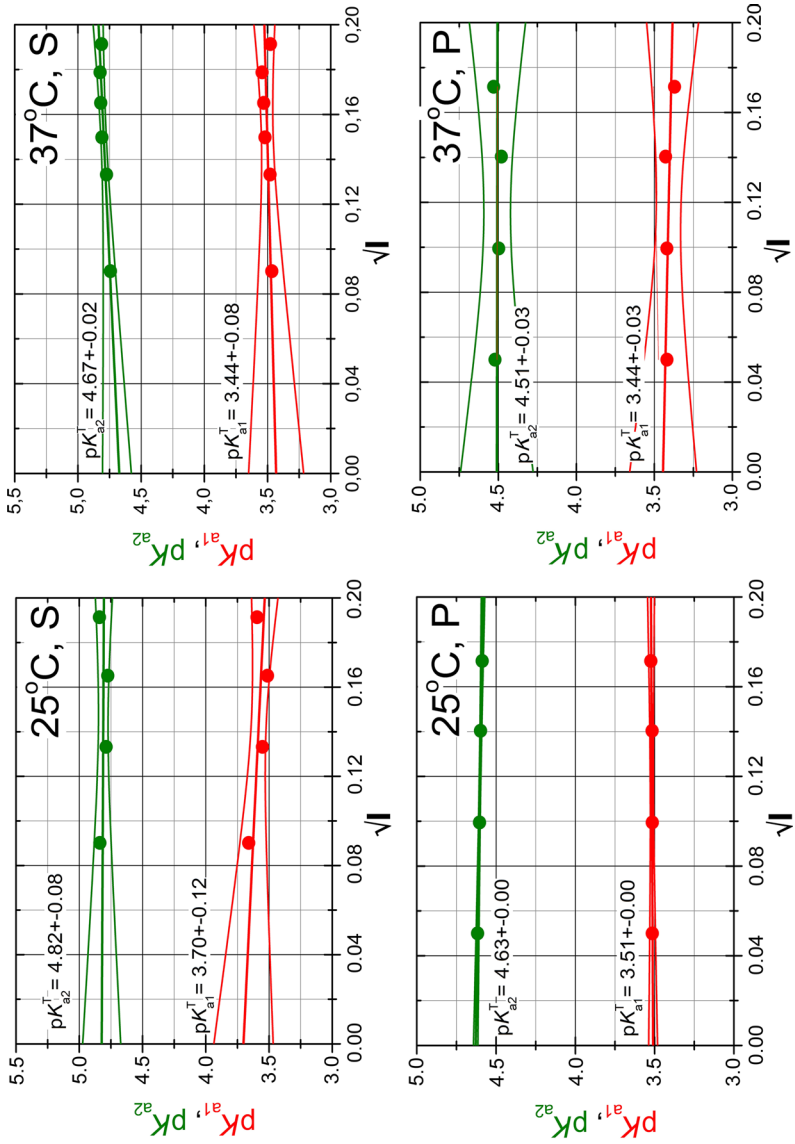

Fig. 8 Dependence of the mixed dissociation constants of Valsartan on the square-root of the ionic strength for the two dissociation constants leading to the thermodynamic dissociation constants pK_a^T at 25 °C and 37 °C using the UV-metric (S) and pH-metric techniques (P)

4.2.4 Step 11: Determination of Enthalpy, Entropy and Gibbs Energy for the "Extrathermodynamics" of Dissociation (in Supplementary Material)

The standard state enthalpy change ΔH^0 of the dissociation process was calculated from the van't Hoff equation

$$\mathrm{d}\ln K/\mathrm{d}T = \Delta H^0/RT^2. \tag{2}$$

From the values of standard state Gibbs energy

$$\Delta G^0 = -RT\ln K \tag{3}$$

and ΔH^0, the standard state entropy change

$$\Delta S^0 = \left(\Delta H^0 - \Delta G^0\right)/T \tag{4}$$

can be calculated, where R (ideal gas constant) = 8.314 J·K^{-1}·mol^{-1}, K is the thermodynamic dissociation constant and T is the absolute temperature.

The estimates of dissociation constants from the pH-metric method were used for a calculation of some extra-thermodynamics. Positive enthalpy values $\Delta H^0(\mathrm{p}K_{\mathrm{a1}}) = 10.33$ kJ·mol^{-1}, $\Delta H^0(\mathrm{p}K_{\mathrm{a2}}) = 17.70$ kJ·mol^{-1} showed that the dissociation process is accompanied by heat absorption. Positive value of the Gibbs energy changes are: $\Delta G^0(\mathrm{p}K_{\mathrm{a1}}) = 20.03$ kJ·mol^{-1}, $\Delta G^0(\mathrm{p}K_{\mathrm{a2}}) = 26.43$ kJ·mol^{-1} at 25 °C. The entropy changes for the dissociation process, ΔS^0 at 25 °C and 37 °C are negative ($\Delta S^0(\mathrm{p}K_{\mathrm{a1}}) = -32.56$ J·K^{-1}·mol^{-1}, $\Delta S^0(\mathrm{p}K_{\mathrm{a2}}) = -29.26$ J·K^{-1}·mol^{-1} at 25 °C and $\Delta S^0(\mathrm{p}K_{\mathrm{a1}}) = -30.01$ J·K^{-1}·mol^{-1} and $\Delta S^0(\mathrm{p}K_{\mathrm{a2}}) = -25.92$ J·K^{-1}·mol^{-1} at 37 °C).

5 Discussion

The REACTLAB regression program analyzed the pH-absorbance matrix of 1×10^{-4} mol·dm^{-3} Valsartan and quantified estimates of two dissociation constants with different numerical approaches. The results of protonation/dissociation constant refinement might include information concerning the goodness of fit of the residual-sum-of-squares function *RSS*, the parameter estimates calculated, the standard deviations on parameters and the correlation coefficients between them, the residuals map, and the concentrations of all the species in the model for all data points. The model selection [36] was the process of deciding whether to accept the results. Usually all of the above factors should be taken into account, since no one of them on its own was a reliable indicator of the success or failure of the calculation.

The ESAB program, minimizing the residuals $e_i = V_{\mathrm{exp},i} - V_{\mathrm{calc},i}$ reached residual values of about 0.1 or 0.2 μL, indicating an excellent curve fitting of the calculated titration curve through the experimental points. It could be stated that the reliability of dissociation constants of Valsartan has been proven, although the group parameters L_0 and H_T were ill-conditioned in the nonlinear regression model. The curve fitting showed sufficient reliability of the estimates of both dissociation constants of Valsartan at 25 and 37 °C.

The inconsistency of the experimentally ascertained $\mathrm{p}K_{ai}$ estimates and their theoretically predicted values could be due to the complicated structure of the heterocyclic nucleus resonance, and consequently to different electron distributions, which might further lead to different predicted $\mathrm{p}K_{ai}$ values according to the structural formula of the molecule. In such cases, the prognostic programs MARVIN, PALLAS and ACD/Percepta might fail, and the

dissociation constants would definitely need to be determined experimentally. Given that the pK_{ai} estimates from both potentiometric and spectrophotometric methods are similar and, most importantly, plausible in terms of achieved fitting in data regression, it can be concluded that the experimental results obtained are reliable and show the real dissociation of the substance.

(1) When pK_a is positive, the standard Gibbs energy change ΔG^0 for the dissociation reaction is also positive. The positive value of the ΔH^0 indicates that dissociation process is endothermic and is accompanied by absorption of heat. The hydrogen bond rearrangement, then, could underlie both ΔH^0 and ΔS^0 in drug–proton interactions and an interrelationship between ΔH^0 and ΔS^0 seems plausible, indeed likely. The hydrogen bond as central to a drug–proton interaction also is mechanistically appealing. In water, the hydrogen bonds form a network of continuous chains that are dynamically changing (in a sort of steady state). Because of the dipole created by displacement of the electron from the hydrogen proton, these chains form a sequence of mono- and di-poles that are sensitive to the electrostatic potential of the drug and receptor molecules and provide a mechanism for transmitting information at a distance from drug to receptor.
(2) The entropy contribution is mostly unfavorable ($\Delta S^0 < 0$) in these reactions. Ions in an aqueous solution tend to orient the surrounding water molecules, which orders the solution and decreases the entropy. The contribution of an ion to the entropy is the partial molar entropy which is often negative, especially for small or highly charged ions. The ionization of an acid involves reversible formation of two ions so that the entropy decreases ($\Delta S^0 < 0$). There are now two anions on the reversible ionization so the entropy again only decreases.

6 Conclusion

(1) Spectrophotometric and potentiometric pH titration allowed the measurement of two close dissociation constants of Valsartan (Scheme 1). Valsartan chromophores exhibited minimal changes of absorbance in UV–Vis spectra when adjusting the pH of the solution, and therefore estimates of dissociation constants were subject to greater uncertainty than from potentiometric determination. For this reason, a more reliable estimation of the dissociation constants was obtained potentiometrically.
(2) Valsartan marked L^{2-} was capable of protonation in pure water to form soluble species LH_2, LH^- and L^{2-}. The graph of the molar absorption coefficients of differently protonated species against the wavelength indicated that the spectrum of ε_L, ε_{LH}, ε_{LH2} were for species correlated, and that the values in pairs are almost the same.
(3) It has been demonstrated that in the range of pH = 2 to 7, two dissociation constants could be reliably estimated from the spectra when the concentration of the sparingly soluble Valsartan was 1.0×10^{-4} mol·dm^{-3} or less. Although adjusted pH less affected the absorbance changes in the chromophore, two thermodynamic dissociation constants were reliably determined, with REACTLAB reaching values of $pK_{a1}^T = 3.70 \pm 0.12$, $pK_{a2}^T = 4.82 \pm 0.08$ at 25 °C and $pK_{a1}^T = 3.44 \pm 0.08$, $pK_{a2}^T = 4.67 \pm 0.02$ at 37 °C.
(4) The two thermodynamic dissociation constants of Valsartan were determined by regression analysis of potentiometric pH-titration curves at a concentration of

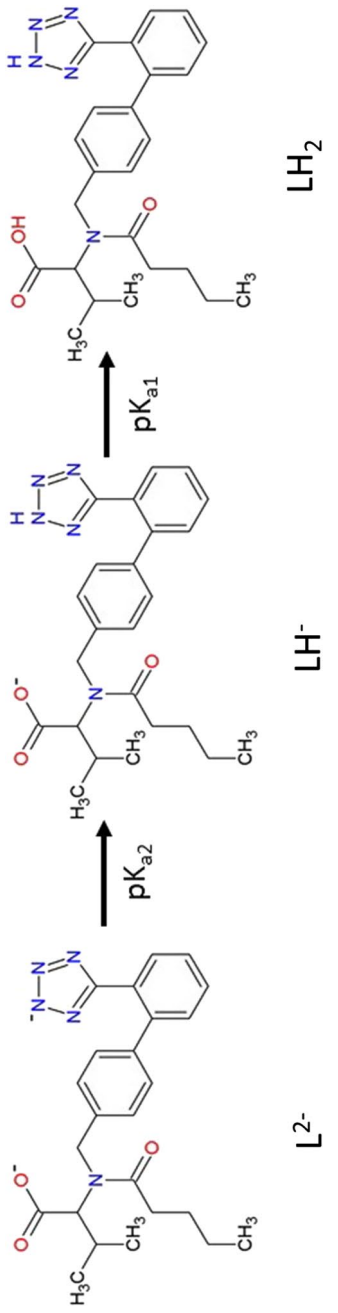

Scheme 1 Protonation scheme of Valsartan

1×10^{-3} mol. dm^{-3} with ESAB, $pK_{a1}^{T} = 3.51 \pm 0.00$, $pK_{a2}^{T} = 4.63 \pm 0.00$, at 25 °C and $pK_{a1}^{T} = 3.44 \pm 0.03$, $pK_{a2}^{T} = 4.51 \pm 0.03$ at 37 °C.

(5) Prediction of the dissociation constants of Valsartan was performed by the programs MARVIN, PALLAS and ACD/Percepta to determine protonation sites. When comparing three predictive and two experimental techniques, prognostic programs sometimes differed in the pK_a estimate.

(6) Thermodynamic parameters ΔH^0 and ΔG^0 were calculated from the temperature change of dissociation constants according to the van't Hoff equation. Positive enthalpy values $\Delta H^0(pK_{a1}) = 10.33$ kJ·mol^{-1}, $\Delta H^0(pK_{a2}) = 17.70$ kJ·mol^{-1} showed that the dissociation process was endothermic and is accompanied by heat absorption. Positive values of the Gibbs energy are $\Delta G^0(pK_{a1}) = 20.03$ kJ·mol^{-1}, $\Delta G^0(pK_{a2}) = 26.43$ kJ·mol^{-1} at 25 °C. The standard state entropies of dissociation, ΔS^0, at 25 °C and 37 °C are negative ($\Delta S^0(pK_{a1}) = -32.56$ J·K^{-1}·mol^{-1}, $\Delta S^0(pK_{a2}) = -29.26$ J·K^{-1}·mol^{-1} at 25 °C and $\Delta S^0(pK_{a1}) = -30.01$ J·K^{-1}·mol^{-1}, $\Delta S^0(pK_{a2}) = -25.92$ J·K^{-1}·mol^{-1} at 37 °C.

References

1. Grujić, M., Popović, G., Nikolic, K., Agbaba, D.: Protolytic equilibria of sartans in micellar solutions of differently charged surfactans. J. Pharm. Sci. **105**(8), 2444–2452 (2016)
2. Lemke, T.L., Williams, D.A., Roche, V.F., Zito, S.W.: Foye´s Principles of Medicinal Chemistry. Lippincott Williams and Wilkins, Philadelphia (2013)
3. Doulton, T.W., He, F.J., MacGregor, G.A.: Systematic review of combined angiotensin–converting enzyme inhibition and angiotensin receptor blockade in hypertension. Hypertension **45**, 880–886 (2005)
4. Brunton, L.L., Chabner, B., Knollmann, B.C.: Goodman and Gilman's The Pharmacological Basis of Therapeutics. McGraw-Hill, New York (2011)
5. Inzucchi, S.E., Bergenstal, R.M., Buse, J.B., Diamant, M., Ferrannini, E., Nauck, M., Peters, A.L., Tsapas, A., Wender, R.: Management of hyperglycemia in Type 2 diabetes, 2015: a patient-centered approach: update to a position statement of the American diabetes association and the european association for the study of diabetes. Diabetologia **55**(6), 1577–1596 (2015)
6. Katzung, B.G., Masters, S.B., Trevor, A.J.: Basic and Clinical Pharmacology, Chapter 11, vol. 13. McGraw-Hill Education, New York (2012)
7. Manallack, D.T., Prankerd, R.J., Nassta, G.C., Ursu, O., Oprea, T.I., Chalmers, D.K.: A chemogenomic analysis of ionization constants–implications for drug discovery. Chem. Med. Chem. **8**, 242–255 (2013)
8. De Stefano, C., Princi, P., Rigano, C., Sammartano, S.: Computer analysis of equilibrium data in solution ESAB2M: an improved version of the ESAB program. Annali Di Chimica **77**(7–8), 643–675 (1987)
9. Gans, P., Sabatini, A., Vacca, A.: Hyperquad computer-program suite. Abstr. Pap. Am. Chem. Soc. **219**, U763–U763 (2000)
10. Gans, P., Sabatini, A., Vacca, A.: Simultaneous calculation of equilibrium constants and standard formation enthalpies from calorimetric data for systems with multiple equilibria in solution. J. Solution Chem. **37**(4), 467–476 (2008)
11. Meloun, M., Havel, J., Högfeldt, E.: Computation of solution equilibria: a guide to methods in potentiometry, extraction, and spectrophotometry. Ellis Horwood series in analytical chemistry. Ellis Horwood, Chichester (1988)
12. Meloun, M., Militký, J., Forina, M.: PC-Aided Regression and Related Methods. Chemometrics for Analytical Chemistry, vol. 2. Ellis Horwood, Chichester (1994)
13. Meloun, M., Militký, J., Forina, M.: PC-Aided Statistical Data Analysis. Chemometrics for Analytical Chemistry, vol. 1. Ellis Horwood, Chichester (1992)

14. Allen, R.I., Box, K.J., Comer, J.E.A., Peake, C., Tam, K.Y.: Multiwavelength spectrophotometric determination of acid dissociation constants of ionizable drugs. J. Pharm. Biomed. Anal. **17**(4–5), 699–712 (1998)
15. Hartley, F.R., Burgess, C., Alcock, R.M.: Solution Equilibria. Ellis Horwood, Chichester (1980)
16. Leggett, D.J., McBryde, W.A.E.: General computer program for the computation of stability constants from absorbance data. Anal. Chem. **47**(7), 1065–1070 (1975)
17. Kankare, Jouko J.: Computation of equilibrium constants for multicomponent systems from spectrophotometric data. Anal. Chem. **42**(12), 1322–1326 (1970)
18. ACD/Labs p*K*a Predictor 3.0. In: Inc., A.C.D. (ed.). Toronto, Canada (2011)
19. Balogh, G.T., Gyarmati, B., Nagy, B., Molnar, L., Keseru, G.M.: Comparative evaluation of in silico pK_a prediction tools on the gold standard dataset. QSAR Comb. Sci. **28**(10), 1148–1155 (2009)
20. Balogh, G.T., Tarcsay, A., Keseru, G.M.: Comparative evaluation of pK_a prediction tools on a drug discovery dataset. J. Pharm. Biomed. Anal. **67–68**, 63–70 (2012)
21. Ribeiro, A.R., Schmidt, T.C.: Determination of acid dissociation constants (pK_a) of cephalosporin antibiotics: computational and experimental approaches. Chemosphere **169**, 524–533 (2017)
22. ChemAxon: MarvinSketch 16.5.2.0. In, vol. 16.5.2.0. ChemAxon, Budapest, Hungary (2013)
23. Hansen, N.T., Kouskoumvekaki, I., Jorgensen, F.S., Brunak, S., Jonsdottir, S.O.: Prediction of pH-dependent aqueous solubility of druglike molecules. J. Chem. Inf. Model. **46**(6), 2601–2609 (2006)
24. Liao, C.Z., Nicklaus, M.C.: Comparison of nine programs predicting p*K*(a) values of pharmaceutical substances. J. Chem. Inf. Model. **49**(12), 2801–2812 (2009)
25. Manchester, J., Walkup, G., Rivin, O., You, Z.P.: Evaluation of p*K*(a) estimation methods on 211 drug like compounds. J. Chem. Inf. Model. **50**(4), 565–571 (2010)
26. Meloun, M., Bordovska, S., Syrovy, T., Vrana, A.: Tutorial on a chemical model building by least-squares non-linear regression of multiwavelength spectrophotometric pH-titration data. Anal. Chim. Acta **580**(1), 107–121 (2006)
27. Meloun, M., Pilařová, L., Bureš, F., Pekárek, T.: Multiple dissociation constants of the interpirdine hydrochloride using regression of multiwavelength spectrophotometric pH-titration data. J. Mol. Liq. **261**, 480–491 (2018)
28. Meloun, M., Čápová, A., Pilařová, L., Pekárek, T.: Multiwavelength UV-metric and pH-metric determination of the multiple dissociation constants of the Lesinurad. J. Pharm. Biomed. Anal. **158**, 236–246 (2018)
29. Meloun, M., Nečasová, V., Javůrek, M., Pekárek, T.: The dissociation constants of the cytostatic bosutinib by nonlinear least-squares regression of multiwavelength spectrophotometric and potentiometric pH-titration data. J. Pharm. Biomed. Anal. **120**, 158–167 (2016)
30. Meloun, M., Syrový, T., Bordovská, S., Vrána, A.: Reliability and uncertainty in the estimation of p*K* (a) by least squares nonlinear regression analysis of multiwavelength spectrophotometric pH titration data. Anal. Bioanal. Chem. **387**(3), 941–955 (2007)
31. Meloun, M., Ferenčíková, Z.: Enthalpy–entropy compensation for some drugs dissociation in aqueous solutions. Fluid Phase Equilibra **328**, 31–41 (2012)
32. Maeder, M., King, P.: Analysis of Chemical Processes, Determination of the Reaction Mechanism and Fitting of Equilibrium and Rate Constants. In: Varmuza, K. (ed.) InTech, London (2012)
33. Meloun, M., Čapek, J., Mikšík, P., Brereton, R.G.: Critical comparison of methods predicting the number of components in spectroscopic data. Anal. Chim. Acta **423**(1), 51–68 (2000)
34. ORIGIN. OriginLab Corporation, One Roundhouse Plaza, Suite 303, Northampton, MA 01060, USA
35. Meloun, M., Militký, J.: Statistical Data Analysis: A Practical Guide, Complete with 1250 Exercises and Answer Key on CD, 1st edn. Woodhead Publishing Ltd., New Delhi (2011)
36. Meloun, M., Bartos, M., Högfeldt, E.: Multiparametric curve fitting.13. Reliability of formation-constants determined by analysis of potentiometric titration data. Talanta **35**(12), 981–991 (1988)